

Cerebral Sinus and Venous Thrombosis in Rats Induces Long-Term Deficits in Brain Function and Morphology—Evidence for a Cytotoxic Genesis

Kai U. Frerichs, Maria Deckert, Oliver Kempfski, Ludwig Schürer, *Karl Einhüpl, and Alexander Baethmann

*Institute for Surgical Research and *Department of Neurology, Klinikum Grosshadern, Ludwig-Maximilians-University Munich, Munich, Germany*

Summary: The pathophysiology of cerebral venous infarctions is poorly understood, due partially to the lack of a suitable experimental model. Therefore, we developed a model in rats to study acute and long-term changes of brain function and morphology following thrombosis of the superior sagittal sinus. The superior sagittal sinus of rats was exposed, ligated, and injected with thrombogenic material. Thrombosis of the longitudinal sinus and ascending cortical veins was monitored by intravital fluorescence angiography. Histology was studied at 24 h and 4 weeks after thrombosis and changes in intracranial pressure, electroencephalogram (EEG), and tissue impedance were noted. Spontaneous locomotor activity was followed for 4 weeks after thrombosis. The effect of heparin treatment on tissue impedance was evaluated. Thrombosis of the superior sagittal sinus could be regularly induced, although pathological sequelae developed only if ascending veins were affected. Sinus and venous thrombosis was histologically characterized by bilateral, parasagittal infarctions. Thrombosis induction was followed by an increase in intracranial pressure from 4.7 ± 1.6 to 12.8 ± 2.4 mm Hg ($n = 4$) at 1 h after thrombosis,

associated with an exponential rise in tissue impedance to $165 \pm 14\%$ ($n = 8$) of the control. EEG changes were similar to those following global cerebral ischemia and remained pathological for up to 6 months after thrombosis ($n = 6$). As a permanent behavioral deficit spontaneous locomotor activity was reduced to $60 \pm 10\%$ ($n = 6$) of the control. Finally, the administration of heparin (1 IU/g body weight) after thrombosis induction was found to reverse the pathological tissue impedance response of the brain. In conclusion, involvement of ascending cortical veins following sinus thrombosis appears to be critical for the development of irreversible tissue damage, such as infarction. Changes in intracranial pressure and tissue impedance suggest that the venous thrombosis was followed by brain edema of a predominantly cytotoxic nature. Venous thrombosis led to long-term changes of brain function, as demonstrated by persistent disturbances of the EEG or of the spontaneous locomotor drive. These deficits may be amenable to treatment with heparin. **Key Words:** Behavior—Cerebral ischemia—EEG—Impedance—Rat—Sinus thrombosis.

The significance of cerebral venous thrombosis as a nonarterial cause of stroke has traditionally been underestimated (Krayenbühl, 1966; Reddy and Rao, 1968; Nagpal, 1983; Boussier et al., 1985; Einhüpl et al., 1990). Most frequently affected are

the superior sagittal sinus (SSS) and ascending cortical veins. Clinical diagnosis is difficult due to the diversity of symptoms. Introduction of serial cerebral angiography made it possible to establish a definite diagnosis of this disease and revealed that milder clinical courses are more common than previously thought. The etiology of sinus and venous thrombosis (SVT) is probably nonspecific, similar to the etiology of venous thrombosis in other parts of the circulation. The pathophysiology of SVT remains obscure, due partly to the considerable variability of the clinical symptoms as a major obstacle of systematic clinical investigations. Various attempts have been made to develop a reproducible

Received May 24, 1993; final revision received August 23, 1993; accepted September 20, 1993.

Address correspondence and reprint requests to Dr. K. U. Frerichs at Division of Neurosurgery, Brigham and Women's Hospital, Harvard Medical School, 75 Francis Street, Boston, MA 02115, U.S.A.

Abbreviations used: CSF, cerebrospinal fluid; EEG, electroencephalogram; ICP, intracranial pressure; MAP, mean arterial pressure; SSS, superior sagittal sinus; SVT, sinus and venous thrombosis.

and clinically relevant animal model of SVT. Although many of these studies succeeded in occluding the SSS, neuropathological consequences were only rarely observed. Besides, it cannot be excluded that part of the observed pathology, including the high mortality, has been artificially induced by the various techniques, such as injection into the SSS of sclerosing agents, e.g., cyanoacrylate (Fujita et al., 1984), ethanalamine (Beck and Russell, 1946), sodium morrhuate (Heinz et al., 1972), lard oil (Putnam, 1935; Woolf, 1954), and hot paraffin (Owens et al., 1957). Other attempts include heat coagulation of the SSS at multiple sites (Sato et al., 1983), tamponade with autologous muscle or cotton (Beck and Russell, 1946) soaked in *Escherichia coli* filtrate for induction of a localized Shwartzman reaction, or the combination of ligation of the SSS and injection of thrombin (Sarwar et al., 1984) into the SSS. Therefore, a model of SVT was developed according to the following guidelines: The method should induce a clinically relevant *thrombosis*, which is regularly survived, allows acute and long-term assessment of pathophysiological alterations of brain function and morphology, and can be established in rats. Such a model may provide a better understanding of the pathophysiology of cerebral venous thrombosis with regard to differences from arterial cerebral ischemia, to the relationship between the extension of thrombosis into ascending veins and the pathological sequelae, to the mechanisms underlying the increase in intracranial pressure (ICP), causing a large part of the mortality, and, most importantly, to therapeutic approaches.

MATERIALS AND METHODS

Surgical preparation

The experiments were carried out in 52 male Wistar rats (346 ± 140 g body weight; Bäumler Inc., Wolfshausen, Germany). The animals were housed at a constant temperature of 21°C, with a light/dark cycle of 12/12 h and free access to food and water. Anesthesia was induced by intraperitoneal injection of 36 mg chloralhydrate/100 g body weight. Atropine (0.5 mg/100 mg body weight) was given intraperitoneally to decrease tracheal secretions. Rectal temperature was monitored and kept constant at 37°C throughout the experiment by a feedback-controlled heating pad. The head was placed into a stereotactic instrument (David Kopf Instruments, Tujunga, CA, U.S.A.) and the calvaria exposed through midline incision. Under the operating microscope, rostral and caudal portions of the SSS were exposed by two small rectangular craniectomies, anterior to the bregma (5×3 mm) and above the torcular Herophili (5×4 mm) (Fig. 1), using a high-speed drill, leaving the dura mater intact. The bone flaps were split in the midline before removal to avoid damage of the SSS. The SSS was ligated rostrally and then caudally close to the confluens sinuum using 9-0 prolene, without damage to the adjacent brain

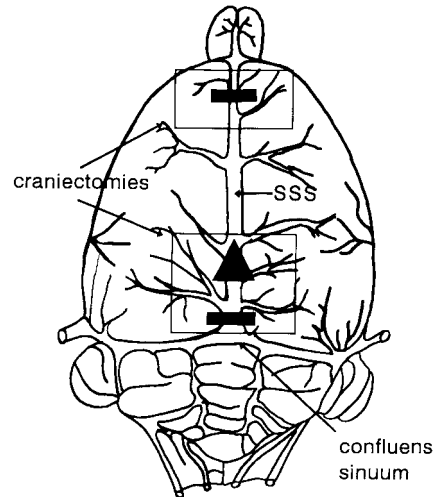


FIG. 1. Dorsal aspect of rat brain and superficial cortical venous system. The SSS was exposed caudally and rostrally by rectangular craniectomies. For SVT induction, the SSS was ligated (bars) rostrally and caudally and then injected with (triangle) a kaolin/cephalin suspension (modified from Zeman and Innes, 1963).

tissue. The distance between the ligatures was ~ 1 cm. A Hamilton microsyringe with a 27-gauge needle attached to a micromanipulator was tangentially inserted into the SSS between the sutures, just rostral to the confluens sinuum. Thrombosis was induced by the injection of 100 μ l of a kaolin/cephalin suspension (PTT reagent; Boehringer, Mannheim, Germany) in fractionated 10- μ l portions at 30-s intervals. Subsequently, the needle was removed without bleeding and the resected bone flaps were repositioned. Saline solution (0.9%) was injected in one animal. In another control group the sinus puncture was omitted to allow recovery to study the electroencephalogram (EEG) and spontaneous activity. Skin closure was done with 4-0 silk.

Fluorescence angiography and histology

In seven rats a PE 50 catheter was inserted into the right femoral vein for injection of 20% sodium fluorescein/100 g body weight prior to the induction of SVT for epicortical angiography and studies of the blood-brain barrier (Wahl et al., 1983; Unterberg et al., 1988). For these experiments, the craniectomy was enlarged to expose the SSS between the sutures for observation of the contributory ascending veins. A photomicroscope (M 400; Wild, Heerbrugg, Switzerland) furnished with a 50-W mercury lamp and a fluorescence filter (I2; Leitz, Wetzlar, Germany) was used for fluorescence angiography, which was carried out before, during, and up to 2 h after induction of SVT ($n = 6$) or sham operation ($n = 1$). The animals were killed at 24 h after SVT for histological evaluation of all experimental groups except the impedance and ICP groups. The animals were killed with pentobarbital (5 mg/100 g body weight). In vivo perfusion was made through the left ventricle, beginning with normal saline containing 10 IU heparin/ml for 2 min, followed by 10% buffered formalin (pH 7.4) for 4 min. The brains were removed, kept in fresh fixative overnight, and then embedded in paraffin. Serial coronal sections (10 μ m) were cut at 400- μ m intervals and stained with hematoxylin and eosin.

Electrical impedance and ICP

Combined measurements of the tissue impedance and the ICP were performed in 14 rats. A PE 50 catheter was inserted into the right femoral artery for monitoring of the blood pressure (mean arterial pressure; MAP) and arterial blood gases. A 25-gauge cannula was introduced into the left lateral ventricle [bregma, -0.8 mm; lateral, 1.4 mm; depth, 3.5 mm (Paxinos and Watson, 1986)], which was connected to a Statham transducer for ICP measurements and a Wheatstone bridge (locally made device). The cannula served as a reference electrode for the impedance measurements. A second electrode (25-gauge needle pin) was introduced 2 mm into the parenchyma of the right temporal lobe through a small burr hole. Both impedance electrodes were electrically isolated except for their tips. Correct placement of the ICP cannula was verified by observations of cardiac and respiratory ICP oscillations. Impedance was measured at a frequency of 1000 Hz AC and a voltage of 13 mV in 30 -s to 5 -min intervals by equilibration of the Wheatstone bridge. Under these conditions, the electrical conductance of the brain, the reciprocal value of the impedance, was determined mainly by the extracellular space, owing to the high electrical resistance of cell membranes (Van Harreveld and Ochs, 1956; Van Harreveld, 1972; Baethmann and Van Harreveld, 1973; De Boer et al., 1989). Therefore, changes in tissue impedance were expected to reflect variations in the size of the extracellular compartment in a reciprocal manner. The contribution of the intravascular compartment to the electrical conductance of the brain tissue was considered to be negligible (Van Harreveld et al., 1963). Impedance and ICP were measured before and up to 4 h after the induction of SVT ($n = 14$) or sham operation ($n = 1$). At the end of the experiment, complete global cerebral ischemia was induced by bleeding from the abdominal vessels to monitor the characteristic posts ischemic impedance changes (Van Harreveld and Ochs, 1956). In two additional animals the left femoral vein was catheterized with PE 50 tubing for administration of a heparin solution (1 IU/g body weight) by bolus injection 5 and 30 min, respectively, after the induction of SVT.

EEG

The EEG recordings were successful in 12 rats. Since the EEG is affected by anesthetic agents (Künkel, 1984), the procedure was modified to induce SVT with consciousness maintained, yet all surgical procedures were carried out under anesthesia. On day 1, the SSS was exposed by two craniectomies as described. Four burr holes were drilled in bifrontal and biparietal positions for insertion of silver-plated EEG electrodes, which were fixed and isolated with dental cement. The tip of the electrodes touched the dura, while the peripheral end was externalized through the skin and connected with the EEG cables. The SSS was then ligated rostrally, while the caudal ligature was prepared with a loose double-tie. The ends of the ligature thread were externalized through Teflon tubings (20 gauge), which were fixed onto the skull with dental cement. An indwelling Teflon catheter (25 gauge) was then implanted into the SSS near the torcular, where it was encompassed by the caudal tie, and fastened onto the occipital bone with dental cement. The externalized catheter was occluded by a metal wire and protected by a plastic cylinder of 1 -cm diameter sutured to the skin of the posterior neck. SVT ($n = 11$) was induced 24 h following recovery in the awake animals by closure of the

caudal ligature and fractionated injection of the thrombogenic material through the implanted sinus catheter. A sham operation was performed in one rat. The cortical EEG was recorded with an eight-channel EEG recorder (Mingograph; Siemens Co., Munich, Germany) before, during, and up to 6 h ($n = 11$) and 6 months ($n = 1$), respectively, after the induction of SVT. Quantitative analysis of the EEG recordings was carried out by digitalization of the analog data and fast Fourier transformation by computer (PDP 11/34; Digital Equipment Co., Munich, Germany). Off-line power spectrography of different EEG frequency bands (KODIAN software; F. X. Mayer Co., Munich, Germany) was made in the following frequency ranges: delta, 1.5 – 3 Hz; theta, 4.5 – 6 Hz; alpha₁, 9 – 10.5 Hz; alpha₂, 12 – 13.5 Hz; beta₁, 15 – 16.5 Hz; beta₂, 21 – 22.5 Hz; and beta₃, 28.5 – 30 Hz (West et al., 1982). Two EEG leads could be stored by the computer simultaneously. Periods of 60 s each were divided into 2.56 -s epochs, with a digital scanning interval of 10 ms. The power of each frequency band was expressed as square microvolts per hertz.

Spontaneous locomotor activity

For quantitation of the spontaneous locomotor drive, 15 rats were placed in activity cages, which consisted of a revolving drum (diameter, 34 cm) and a living compartment for food and water uptake ($27.5 \times 15 \times 12$ cm). Revolutions of the drum were registered by computer (Kontron PC; Kontron Co., Eching, Germany) at 4 -min intervals. The activity cages were isolated from external stimuli, such as noise and movements, and kept under a constant room temperature and humidity with a $12/12$ -h light/dark cycle. Spontaneous running was measured for a control period of 3 weeks prior to the induction of SVT and for 4 weeks following SVT ($n = 11$) or sham operation ($n = 4$), before the brains were removed for histological examination. A consistent pattern and level of wheel running were established by the tenth day or not at all, in which case the animal was excluded from the experiment. After this time span, intraindividual variability was negligible.

Statistical analysis

Data are expressed as the mean value \pm standard deviation. Two-tailed Student's t statistics were used for analysis of unpaired data. The Wilcoxon matched-pairs test was used for paired data. p values <0.05 were accepted as statistically significant.

RESULTS

Intravital fluorescence angiography and histology

The combination of ligation of the SSS rostrally and caudally with injection of thrombogenic material into the SSS, but not ligation alone, caused thrombosis of the SSS. Thrombosis was visible by engorgement and darkening of the SSS. The thrombotic occlusion was effectively preventing any bleeding from the SSS injection site. Extension and spread of the thrombotic occlusion could be observed on fluorescence angiography. Moving blood cells were visible at high power as dark particles against the fluorescing background. Ligatures alone

produced a reduction of blood flow within the SSS but no cessation of flow, although drainage via the confluens sinuum was completely obstructed. Upon additional injection of the kaolin/cephalin suspension, however, thrombotic occlusion of the SSS developed in all experimental animals. In three rats, thrombosis spread beyond the SSS into ascending cortical veins. In the remaining three rats, thrombosis was limited to the SSS. Blood flow in the ascending veins seemed unimpaired, although the direction of flow was reversed, indicative of opening of collateral pathways. Spotty extravasation of fluorescein occurred in the vicinity of larger cortical veins shortly after the induction of thrombosis in the group with additional involvement of ascending veins, while no fluorescein extravasation was observed at the site of the sinus sutures. Histological changes evolved only in the group of animals with the spread of thrombosis into ascending cortical veins (called SVT in the following). At 24 h after SVT (Fig. 2A), bilateral, parasagittal zones of infarction were seen in hematoxylin/eosin-stained sections. Serial sections revealed the extension of these changes. Figure 3 shows schematically the spread of venous infarction in a coronal and longitudinal plane. The location of the necrotic regions is consistent with the SSS-dependent drainage areas (Zeman and Innes, 1963; Hassler, 1966; Schumacher, 1984) and in agreement with findings in human autopsy material (Krayenbühl, 1966). The thrombosed vessels showed the features of red fibrin thrombus formation. Dead neurons could be observed throughout all cortical layers within the necrotic area (Fig. 2B). Rarefaction of the neuropil and of perivascular spaces also occurred in the corpus callosum and hippocampus. Occasionally, perivascular red blood cell extravasation was observed. At 4 weeks after SVT ($n = 6$), the necrotic areas had undergone regressive changes and were eventually being absorbed and replaced by cerebrospinal fluid (CSF)-filled spaces. The lateral ventricles appeared to be slightly enlarged.

Tissue impedance, ICP, and systemic physiological changes

Induction of SVT was followed by an exponential increase in tissue impedance (Fig. 4), reaching an elevated plateau after approximately 20 min, accompanied by a more gradual increase in ICP, from a control level of 6.2 to 11 mm Hg at 60 min in this experimental animal. One hour after SVT induction, global cerebral ischemia induced by exsanguination caused an additional exponential impedance increase, reaching a maximum after only 3–5 min, as described previously in models of cardiac arrest

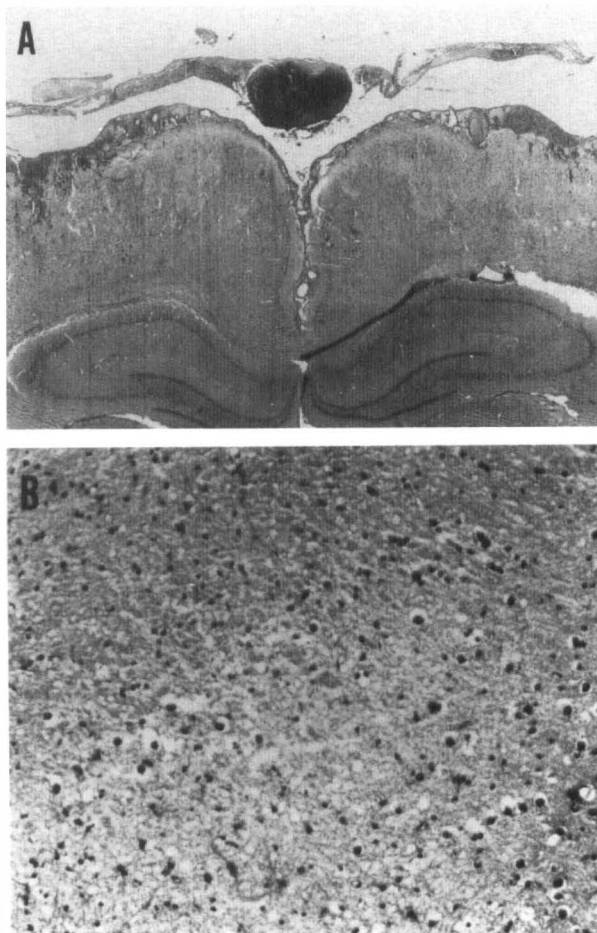


FIG. 2. Coronal hematoxylin & eosin-stained section of a rat brain 24 h after induction of SVT (millimeter scale) demonstrating parasagittal and biparietal infarctions in low-power (A) and high-power (B) views of the infarcted cortex. The thrombosed SSS and small perivenular hemorrhages can be seen in A. All neurons in the infarcted region are necrotic (B). (A) $\times 90$ and (B) $\times 250$.

or global cerebral ischemia (Van Harreveld, 1956; Van Harreveld, 1972). An increase in tissue impedance after SVT could be induced in eight of 14 animals (Fig. 5). The maximal impedance change after SVT reached $80 \pm 14\%$ of the impedance response following global cerebral ischemia. In two animals, impedance was followed for 4 h after SVT without any further changes.

Simultaneous ICP measurements were successfully performed in four animals in this group ($n = 7$). The ICP showed a gradual increase, from a control value of 4.7 ± 1.6 to 12.8 ± 2.4 mm Hg ($p < 0.05$; $n = 4$) 60 min following SVT. This may correspond to an increase in the intracranial volume of approximately 50–100 μ l in the rat skull or 50–100 ml in the human (Kingman et al., 1988). In the remaining six rats as well as in the sham-operated animal, neither impedance nor ICP (5.2 ± 2 -mm Hg

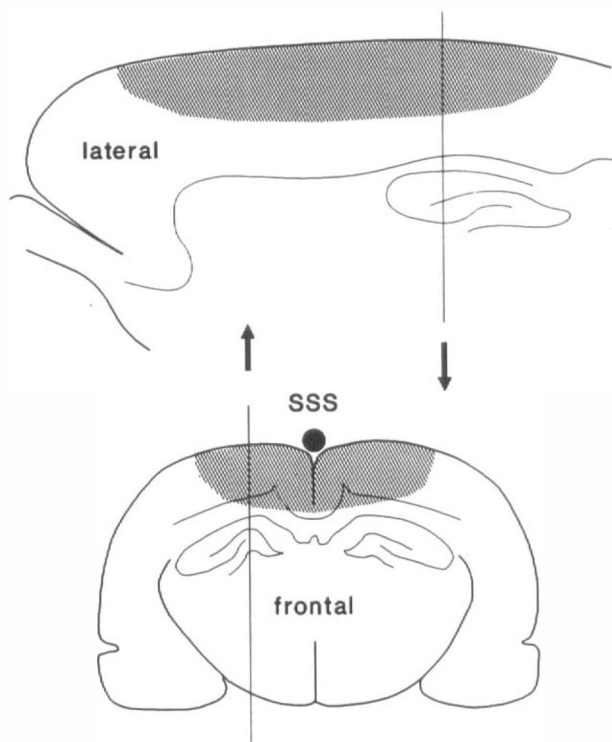


FIG. 3. Schematic view of a lateral (**top**) and a coronal (**bottom**) section through the rat brain. Arrows indicate the anatomical levels of the respective sections. Extension of pathological changes following SVT as assessed in serial sections is indicated by the shaded area.

control vs. 6.4 ± 3.6 mm Hg at 60 min, n.s.; $n = 3$) showed any significant variation from baseline within an observation period of up to 120 min following injection of the thrombogenic material. Global cerebral ischemia by bleeding in these animals, however, led to the characteristic exponential impedance response described above, thereby validating the preceding experiments. In all animals, injection of the thrombogenic material was followed by a 5- to 15-min-duration decrease in blood pressure and change in arterial blood gases and pH (Table 1). No significant differences were seen between animals with (group A) and animals without (group B) a pathological impedance and ICP response, except for the duration of the MAP decrease, which lasted 12.5 ± 3.7 min in group A ($n = 8$) and 7.8 ± 3.1 min in group B ($n = 6$; $p < 0.05$).

EEG and acute behavioral changes

Induction of SVT was successful in 11 animals in the EEG group. Control recordings showed a low-amplitude desynchronized activity in the alpha range. The alpha rhythm was more pronounced in the occipital recordings (Fig. 6). Induction of SVT was followed by transient depression of the EEG activity in all frequency ranges, nearly reaching isoelectricity (Fig. 6; 5-min time point). During this

period, the animals were not comatous but were markedly reduced in their vigilance. The righting reflex was preserved, as well as responses to painful stimuli. The EEG recovered within 30–40 min, then presenting largely delta activity in all recordings. This was associated with improved vigilance. At 4 h after SVT, EEG activity had partially returned also in the higher-frequency ranges (beta and alpha), yet delta activity was still dominant 24 and 50 h after SVT. Such a course could be reproduced in six animals. A quantitative statistical analysis is shown in Fig. 7A (biparietal recording) and Fig. 7B (parasagittal recording). The changes in EEG power over time in the different frequency ranges after SVT are given at representative time points for up to 250 min following thrombosis induction. The baseline data are shown as blank histograms (Fig. 7) throughout the subsequent time points for better comparison. At 10 min after SVT, the EEG power had partially returned but remained significantly depressed at all frequencies except in the delta range. The EEG was subsequently dominated by an increase in the delta power. Although the EEG power also returned in the higher-frequency ranges, no significant change compared to baseline could be detected. Therefore, the overall increase in EEG power (0–30 Hz) could be attributed mainly to changes in the low-frequency bands. In two rats in this group, spike activity (single spikes and polyspike complexes) developed at 3–4 h following SVT but was not associated with clinical signs of seizure activity. In all six animals in this group, histology of the brains at 24 h ($n = 5$) or 6 months ($n = 1$) revealed bilateral pathological changes in the parasagittal region. In the remaining five animals as well as in the sham animal, the injection of thrombogenic material or the sham operation remained without effect on behavior or EEG, which was followed for up to 2 h after injection. Histology at 24 h did not reveal any pathological changes except for a thrombosed SSS.

Spontaneous activity and chronic behavioral changes

None of the experimental animals died or developed any obvious focal neurological symptoms, such as paresis or epileptic seizures, following injection of the thrombogenic material or the sham operation. A circadian rhythm could be observed in all animals, with the majority of activity occurring during the dark phase. Therefore, the running data are expressed as average revolutions per minute during the 12-h dark phase in percent of control (4.73 ± 3.1 rpm; $n = 15$). The induction of SVT decreased the spontaneous running level to ~60%

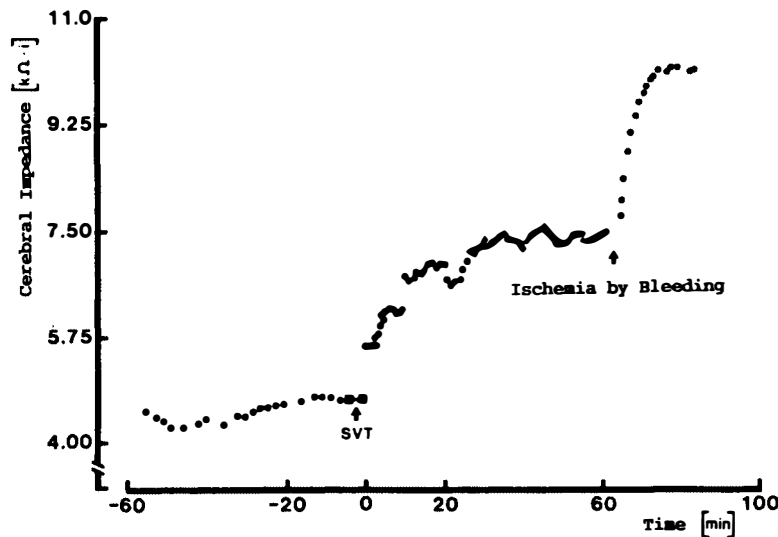


FIG. 4. Acute impedance response of the brain following SVT in an individual experiment. SVT was followed by an exponential impedance increase, reaching a plateau after 20 min. At 60 min, global ischemia was induced, in addition, by bleeding, causing a further rise in impedance, with a maximum response after 5 min. SVT indicates the injection of thrombogenic material.

of the control ($n = 6$) (Fig. 8), without any tendency for recovery within the observation period of 4 weeks after SVT. In the remaining five animals in this group as well as in sham-operated rats ($n = 4$) (Fig. 8), spontaneous running activity recovered rapidly, within days. Histology at 4 weeks after SVT induction revealed bilateral regressive changes in the parasagittal region only in animals with a permanent reduction in running activity. The animals' body weights increased similarly in all groups [Table 2; groups (A) with and (B) without pathological changes and the sham group].

Heparin treatment

Administration of heparin at 5 and 30 min after SVT induction, studied in two experiments, led to a reversal of the resulting brain tissue impedance increase within minutes after injection (Fig. 9). The course of impedance following SVT in eight untreated control animals is shown as the 95% confi-

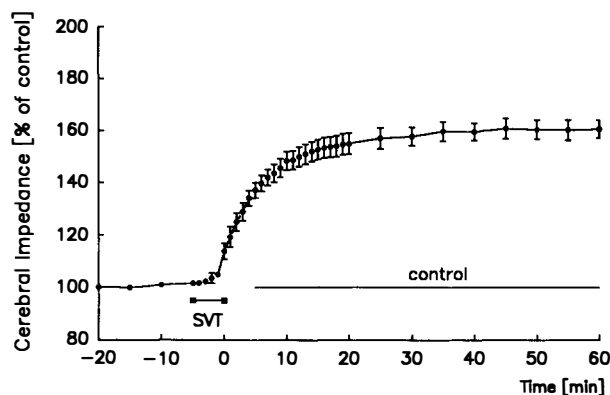


FIG. 5. Acute tissue impedance response following SVT ($n = 8$). Data are expressed as percentage change from baseline. The consistency of the impedance change is underlined by the low variation of the average datum points. SVT indicates the injection of thrombogenic material.

dence limits of the mean. In the animals receiving heparin, the impedance values crossed the lower 95% limit 20–25 min after the onset of treatment. The validity of the impedance measurement was confirmed by the characteristic response to global cerebral ischemia by exsanguination.

DISCUSSION

The present report describes acute and chronic changes in brain function and morphology following experimental SVT in rats. Thrombosis of the SSS could be regularly induced by the combination of ligation of the SSS with injection of thrombogenic material. Thrombotic involvement of the ascending cortical veins, which occurred in about half of the experimental animals, appeared to be essential for any pathology to develop. Histologically, SVT caused parasagittal infarctions. Acutely after SVT, the tissue impedance increased exponentially, accompanied by a rise in the ICP. An acute and transient EEG depression evolving immediately after SVT was followed by a long-lasting slowing of the electrical activity. Further, SVT was characterized

TABLE 1. Arterial blood gases and MAP before and 5 min after SVT

	Group A		Group B	
	Control	5 min	Control	5 min
MAP (mm Hg)	86 ± 8	68 ± 11 ^a	83 ± 7	64 ± 7 ^a
pH	7.37 ± 0.08	7.31 ± 0.08 ^a	7.39 ± 0.10	7.32 ± 0.12 ^a
Po ₂	90 ± 17	68 ± 25 ^a	92 ± 17	73 ± 19 ^a
Pco ₂	29 ± 6	37 ± 14 ^a	25 ± 10	35 ± 15 ^a

Groups indicate the findings in animals with (group A; $n = 8$) and without (group B; $n = 6$) pathological impedance and ICP responses after SVT. Values are means ± SD.

^a $p < 0.05$ (control vs. 5 min within each group).

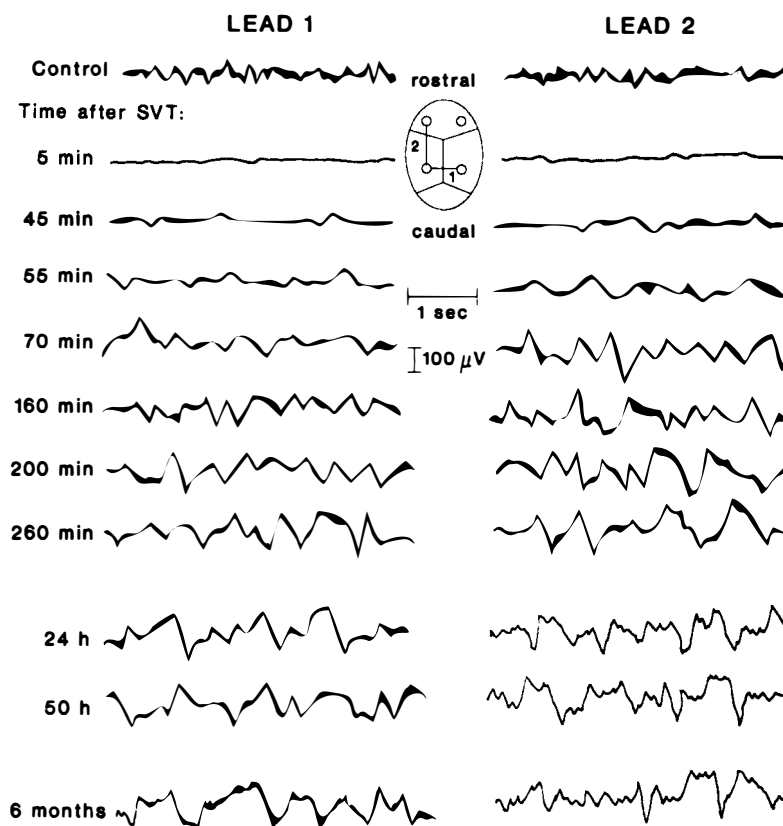


FIG. 6. Acute and chronic changes in the EEG after SVT. The EEG was recorded for up to 6 months in this experimental animal. Lead 1 shows bioccipital and lead two parasagittal tracings. Time and amplitude scales are indicated. The control EEG shows a normal activity of low amplitude in the alpha range. Immediately after SVT induction, the EEG activity was lost in all leads, followed by recovery within 30–40 min, with delta activity then predominating. No tendency to recovery from the pathological delta dominance was observed for up to 6 months after SVT.

by a continuing decrease in the spontaneous locomotor activity. Finally, heparin treatment was found to reverse a pertinent pathological response, namely, the ischemic rise of the specific electric tissue resistance (impedance).

Experimental induction of SVT and importance of ascending cortical vein involvement

Although previous studies succeeded in occluding the SSS by a variety of techniques (Putnam, 1935; Woolf, 1954; Beck and Russell, 1946; Owens et al., 1957; Heinz et al., 1972; Sato et al., 1983; Fujita et al., 1984; Sarwar et al., 1984), they failed to demonstrate consistent or any pathological consequences. When pathological changes were found, the distinction from methodological artifacts, including mortality, was difficult. The purpose of the present experimental method was not only to cause mechanical obstruction, but to induce formation of a fibrin thrombus in the SSS and cortical veins. Thrombosis was triggered by the kaolin/cephalin reagent, which activates the intrinsic pathway of coagulation (Proctor and Rapaport, 1961). Cephalin substitutes for platelet factor 3. Coagulation is precipitated by surface activation by the kaolin particles (diameter, 1–4 μm). The systemic physiological changes immediately following injection might be

attributable to the escape of some of the thrombogenic reagent into the general circulation, causing thrombosis, for example, in the lungs. These changes, however, appeared to be benign and rapidly reversible.

It has been proposed that the involvement of cortical veins might be critical for the development of any neurological deficits in human SVT (Boussier et al., 1985; Einhüpl et al., 1990). Sato et al. (1983) observed a relationship between the involvement of cortical veins and the susceptibility to develop intracranial hemorrhage in a model of heat coagulation of the SSS in dogs. Our data support a relationship between the involvement of cortical veins in SVT and the occurrence of pathological changes. This is based on the following observations. Histo-pathological changes were detected exclusively in animals with acute angiographic extension of the SSS thrombus into ascending cortical veins, which occurred in 50% of the animals in this group ($n = 6$). All other groups, in which fluorescence angiography was not carried out, were split into subgroups at a similar ratio. Fifty-seven percent of the animals with impedance measurements, 55% of the EEG group, and 55% of the group in which spontaneous activity was assessed showed pathological changes of the respective parameter after SVT as well as of

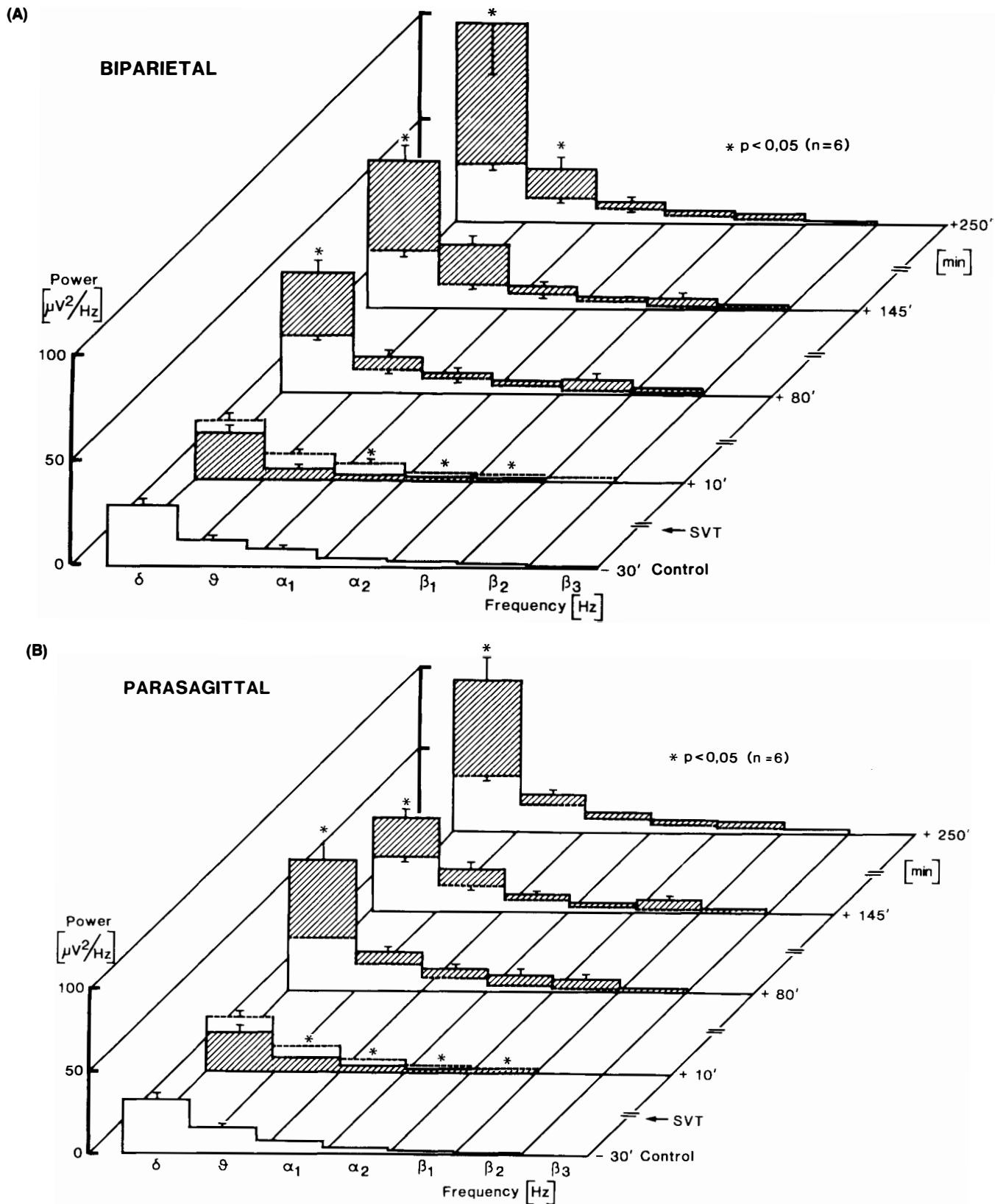


FIG. 7. EEG power spectrographs obtained before and up to 250 min following SVT in biparietal (A) and parasagittal (B) recordings. The changes are shown at representative time points (z axis). The control finding is shown as a blank at subsequent time points (*) $p < 0.05$ vs. control.

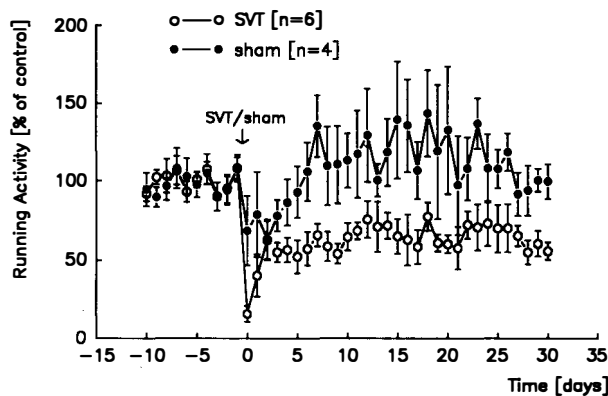


FIG. 8. Spontaneous running activity following SVT (revolutions of the running wheel per minute during the dark period) expressed as percentage of control. Induction of SVT was followed by a decrease in spontaneous wheel running to ~60% of control, without any tendency to recovery within an observation period of 4 weeks. Running activity recovered rapidly in the sham group.

the other parameter, such as histology. No pathological changes in any of the parameters studied were detected in the rest of the animals. The combined average of animals showing concurrent changes in multiple parameters for these three groups was $54.2 \pm 9.7\%$ ($n = 42$). Accordingly, a pathological impedance increase was observed only in animals with a rise in ICP.

Impedance, ICP, and hydrocephalus

Among the most common symptoms in human SVT are headaches and elevated ICP (Bansal et al., 1980; Nagpal, 1983; Bousser et al., 1985). Computerized tomography often reveals compressed cisternal spaces and small ventricles (Buonanno et al., 1978; D'Avella et al., 1980; Einhäupl et al., 1990) in the acute stage of the disease. Intracranial hemorrhages confound the clinical picture in only 10% (Bousser et al., 1985) to 30% (Einhäupl et al., 1990) of cases and were rarely observed in the current model. In severe human cases the ICP may be as high as 72 mm Hg (Hanley et al., 1988). No satisfactory pathophysiological explanation has been offered for this consistent clinical finding. Possible

TABLE 2. Changes in body weight in animals with (group A; $n = 6$) and without (group B; $n = 5$)^a reduction in their spontaneous running activity at days 0 and 30 following induction of SVT or sham operation ($n = 4$)^a

	Sham group	Group A	Group B
Body weight (g)			
Day 0	383 ± 32	370 ± 24	365 ± 29
Day 30	434 ± 30	417 ± 29	415 ± 26
Increase (%)	13 ± 2	13 ± 5	14 ± 4

^a Values are means ± SD.

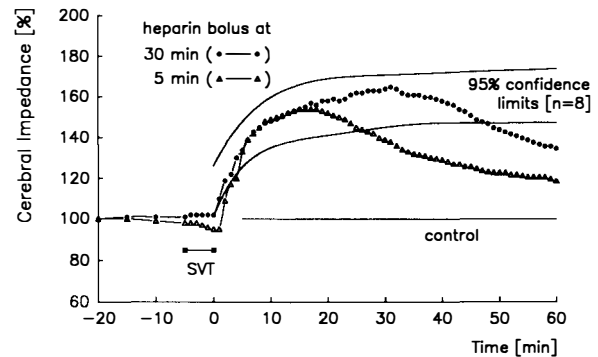


FIG. 9. Effect of administration of heparin (1 IU/g body weight) on the pathologic impedance increase. The impedance change in untreated animals is shown as the 95% confidence limits ($n = 8$) of the mean impedance course (see Fig. 5). As shown, heparin reversed the pathological impedance increase, even if administered 30 min after the induction of SVT.

mechanisms include an increased intracranial blood volume or vasogenic brain edema due to venous congestion. Alternatively, cerebral ischemia by venous flow obstruction may have caused the development of cytotoxic edema. In the current experiments, SVT was followed by a substantial increase in the ICP associated with an exponential rise in the electrical tissue impedance. It has been demonstrated that changes in the cerebral impedance indicate changes in the extracellular fluid space (Van Harreveld, 1972). Hence, an increase in the electrical impedance, i.e., loss of conductivity, is attributable to shrinking of the extracellular space from expansion of the intracellular compartment. Accordingly, the administration of metabolic inhibitors (Baethmann et al., 1973) or induction of global cerebral ischemia (Van Harreveld and Ochs, 1956), which cause cytotoxic cell swelling and thus shrinkage of the extracellular compartment, induce impedance changes strikingly similar to those observed in the present study. Therefore, our data suggest rapid development of cytotoxic edema after SVT, with displacement of fluid from the interstitial to the intracellular compartment, reaching ~80% of the maximal response induced by global cerebral ischemia. In arterial cerebral ischemia, cytotoxic edema does not induce an intracranial volume increase before the onset of reperfusion. In SVT, however, it can be assumed that arterial perfusion continued, providing a basis for net influx of water and early ICP changes. A significant contribution of vasogenic edema or of an increased cerebral blood volume after SVT is unlikely, as both would cause an impedance response in opposite directions. Further, no increase in sodium fluorescein fluorescence was noted within 2 h of thrombosis formation except for occasional spotty extravasation adjacent to

cortical veins. In later stages, SVT in humans as well as in the current model appears to be characterized by enlargement of the cerebral ventricles (Munderloh et al., 1981) and could be due to resorption, i.e., hydrocephalus ex vacuo, or disturbances of the CSF circulation.

EEG

Changes in the EEG are common in patients with SVT, including generalized and focal slow-wave activity and epileptic activity (Boussier et al., 1985; Einhupl et al., 1990). Induction of SVT in awake and unrestrained animals provided nearly ideal conditions for EEG recordings. The sequence of transient isoelectricity followed by a delta-dominated EEG after SVT in the present model is similar to changes observed after transient global ischemia and reperfusion (Pulsinelli and Brierley, 1979; Blomquist and Wieloch, 1985). EEG activity, if adequately quantified, may reflect the postischemic metabolic state of the brain more accurately than assessment of cerebral blood flow (Sulg, 1984). In fact, the duration of EEG isoelectricity, indicative

of absent neuronal activity, has been identified as a prognostic factor of neurological outcome following traumatic and ischemic brain injury (Bricolo et al., 1978; Brierley et al., 1980). Diffuse delta activity, which in the current report dominated the EEG after its recovery from electrical silence, originates in still-viable cortical neurons and may reflect functional disturbances beyond the cortical gray matter (Gloor et al., 1968, 1977), namely, in thalamic nuclei, which are responsible for normal EEG synchronization. Spike activity is also common in arterial ischemia, indicating a worsening prognosis, especially in regions of marginal blood flow such as watershed areas (Chatrian et al., 1968). The persistence of the pathological EEG changes for up to 6 months after SVT might be attributable to structural consolidation of the functional disturbance.

Behavioral deficit

Mortality in SVT is ~10–15% (Boussier et al., 1985; Einhupl et al., 1990) and long-term morbidity is significant as well. On the Glasgow Outcome Scale [0 (death)–5 (normal)], untreated patients

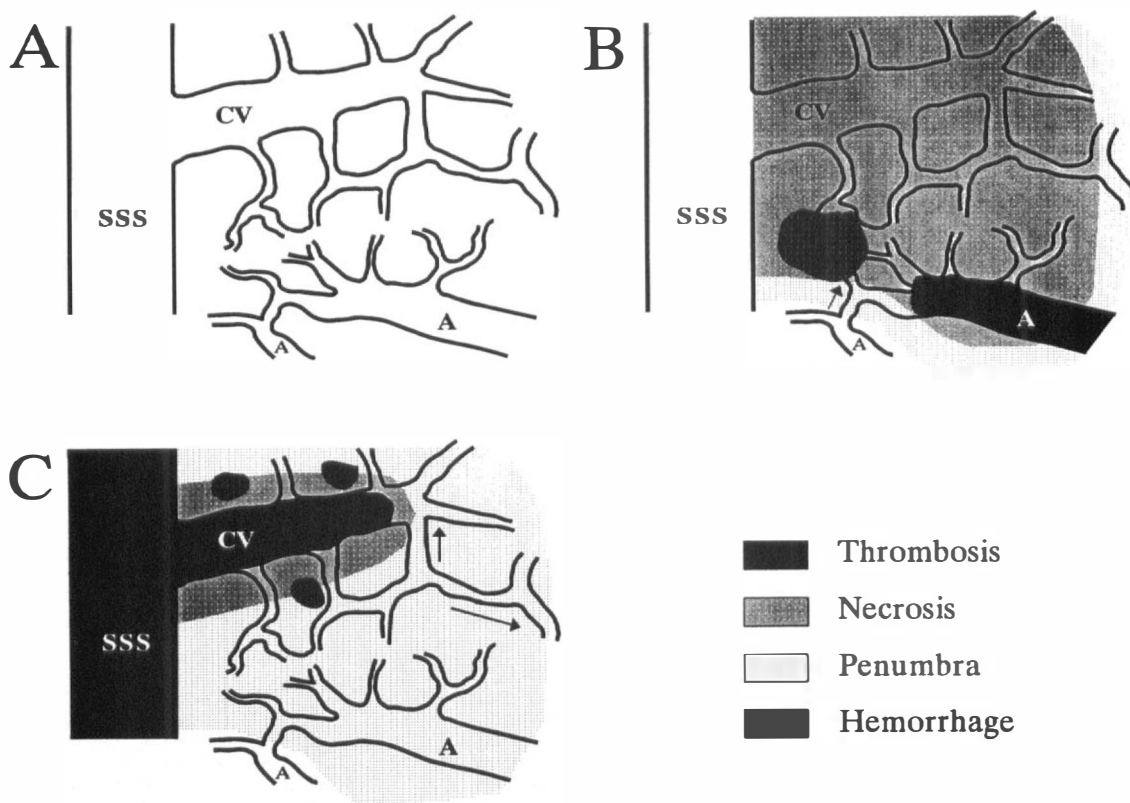


FIG. 10. Pathophysiological concept of infarct formation and development of ischemic brain edema by arterial versus venous blood flow obstruction. **A:** A segment of the vascular bed including a portion of the SSS with an ascending cortical vein (CV). The arterial supply is indicated (**A**; e.g., branch of the middle cerebral artery). **B:** Changes following arterial obstruction. A largely necrotic tissue zone is surrounded by a metastable region, the ischemic penumbra. Collateral blood flow, indicated by the arrow, is insufficient and increases the likelihood of hemorrhage. **C:** In sinus thrombosis with involvement of cortical veins, the area of infarction remains small compared to the extent of functional disturbances in the penumbral zone. Collateral blood flow (arrows) is sufficient to prevent infarction in most of the affected tissue.

reached an average score of only 3 (unable to work but independent at home) 3 months after onset of the disease (Einhäupl et al., 1990). Reduced vigilance is an important factor in morbidity in these patients. In the present study, SVT was followed by a long-term behavioral deficit as shown by the depression of the locomotor drive. In gerbils, brief periods of carotid occlusion may be followed by a phase of hyperactivity reaching a maximum at 24 h postischemia (Chandler et al., 1985; Gerhardt et al., 1986). On the other hand, the depression of spontaneous activity following prolonged ischemia (Chandler et al., 1985) is similar to our observations in experimental SVT. In arterial ischemia, however, the depression of spontaneous activity was associated with a mortality of 42% and extensive histopathology. Measurement of spontaneous wheel running has been shown to be an accurate estimate of the general level of activity (Finger and Mook, 1971). It can be utilized as a valuable indicator of long-term prognosis and functional outcome and may be suitable for studying therapeutic interventions. Depression of the general activity not only may result from widespread brain damage, but also can be produced by isolated lesions of, e.g., the medial septal nuclei or the amygdala (Clody and Carlton, 1969).

Therapy

Anticoagulation in SVT is considered dangerous by some investigators (Barnett and Hyland, 1953; Weber, 1966; Gettelfinger and Kokmen, 1977). Others are in favor of anticoagulation even in the presence of hemorrhage or infarction (Nag and Nadkarni, 1971; Mattes and Dörstelmann, 1981; Bousser et al., 1985; Einhäupl et al., 1991). In a placebo-controlled clinical trial (Einhäupl et al., 1991), morbidity was significantly reduced and the severity of intracranial hemorrhage was diminished in heparin-treated patients ($n = 20$). Our results support a beneficial effect of heparin, as shown by the reversal of the pathologic impedance increase, which could be interpreted as a reduction of cytotoxic edema.

Pathophysiological concept

Confinement of the histopathological changes following SVT to the parasagittal region appears to be in contrast to the severity of the ICP and impedance responses as well as the severity and persistence of the functional deficits. The character and magnitude of these responses are similar to those of responses after prolonged cerebral ischemia. In the case of arterial ischemia, such changes would be associated with a high mortality. A pathophysiological concept is offered to explain this possible dis-

crepancy (Fig. 10). In arterial blockage (Fig. 10B), the tissue is rapidly and irreversibly damaged, resulting in ischemic cell necrosis. Collateral arteries are not able to provide a sufficient blood supply but, in fact, constitute a potential source of hemorrhage. A risk of hemorrhage is also provided by reperfusion into the necrotic area. In venous thrombosis (Fig. 10C), initially only a small part of the cerebral parenchyma may become irreversibly damaged. Perfusion of the affected brain tissue might still be possible at lower flow rates, if the blood flow is drained through collateral pathways. The observation of progressive hypoperfusion estimated by cortical laser Doppler velocimetry following experimental SVT supports this concept (Ungersböck et al., 1993). Such flow conditions, however, may result in functional disturbances, such as cell swelling, once blood flow falls below a critical threshold. Thus, it might be assumed that swollen cells in that region are only functionally, and not irreversibly, damaged and, therefore, have a potential for recovery. Such a tissue area of marginally reduced blood flow has been defined previously as "ischemic penumbra" (Astrup et al., 1981). If, however, venous obstruction progresses or is maintained for longer periods, such a metastable area may also become necrotic. Further, venous congestion, leading to an increased intravascular pressure, may precipitate diapedesis and hemorrhage in a region already at risk from the low-flow conditions. Meaningful relief would be an improvement in the collateral blood flow or reperfusion itself. Since reperfusion would also normalize the increased intravascular pressure, the risk of hemorrhage should decrease as well. Further, anticoagulation with heparin should prevent ongoing thrombosis in the vascular bed affected by venous stasis.

Acknowledgment: The excellent technical assistance of Ms. Ulrike Goerke and Ms. Hilde Fuderer is acknowledged. We thank Professor Jürgen Aschoff (Max Planck Institute for Behavioral Research, Erling/Andechs, Germany) for providing the activity cages and Dr. Christof Garner (Department of Neurology, Munich University, Munich, Germany) for the software for the acquisition of activity data. This work was supported by DFG Grant BA 452/65.

REFERENCES

- Astrup J, Siesjö BK, Symon L (1981) Thresholds in cerebral ischemia—the ischemic penumbra. *Stroke* 12:723–725
- Baethmann A, Van Harreveld A (1973) Water and electrolyte distribution in gray matter rendered edematous with a metabolic inhibitor. *J Neuropathol Exp Neurol* 32:408–423
- Bansal BC, Gupta RR, Prakash C (1980) Stroke during pregnancy and puerperium in young females below the age of 40 years as a result of cerebral venous/venous sinus thrombosis. *Jap Heart J* 21:171–183
- Barnett HJM, Hyland HH (1953) Non-infective intracranial venous thrombosis. *Brain* 76:36–49

- Beck DJK, Russell DS (1946) Experiments on thrombosis of the superior longitudinal sinus. *J Neurosurg* 3:337-347
- Blomquist P, Wieloch T (1985) Ischemic brain damage in rats following cardiac arrest using a long-term recovery model. *J Cereb Blood Flow Metab* 5:420-431
- Boussier MG, Chiras J, Borjes J, Castaigne P (1985) Cerebral venous thrombosis—a case review of 38 cases. *Stroke* 16:199-213
- Bricolo A, Turazzi F, Faccioli F, Odorizzi F, Sciarreta G, Eruliani P (1978) Clinical applications of compressed spectral array in long-term EEG monitoring in comatose patients. *Electroenceph Clin Neurophysiol* 45:211-225
- Brierley JB, Prior PF, Calverley J, Jackson SJ, Brown AW (1980) The pathogenesis of ischaemic neuronal damage along the cerebral arterial boundary zones in Papio anubis. *Brain* 103:929-965
- Buonanno FS, Moody DM, Ball MR, Laster DW (1978) Computed cranial tomographic findings in cerebral sinovenous occlusion. *J Comp Assist Tomogr* 2:281-290
- Chandler MJ, Deleo J, Carney JM (1985) An unanesthetized-gerbil model of cerebral ischemia-induced behavioral changes. *J Pharmacol Meth* 14:137-146
- Chatrjian GE, Shaw CM, Leffmann H (1968) The significance of periodic lateralized epileptiform discharges in EEG: an electrographic, clinical and pathological study. *Electroenceph Clin Neurophysiol* 17:177-193
- Clody DE, Carlton PL (1969) Behavioral effects of lesions of the medial septum of rats. *J Comp Physiol Psychol* 67:344-351
- D'Avella D, Greenberg RP, Mingrino S, Scanarini M, Pardatscher K (1980) Alterations in ventricular size and intracranial pressure caused by sagittal sinus pathology in man. *J Neurosurg* 53:656-661
- De Boer J, Klein HC, Postema F, Go KG, Korf J (1989) Rat striatal cation shifts reflecting hypoxic-ischemic damage can be predicted by on-line impedance measurements. *Stroke* 20:1,377-1,382
- Einhäupl K, Villringer A, Haberl RL, Pfister W, Deckert M, Steinhoff H, Schmiedek P (1990) Clinical spectrum of sinus venous thrombosis. In: *Cerebral Sinus Thrombosis—Experimental and Clinical Aspects* (Einhäupl K, Kempfski O, Baethmann A, eds.), New York, Plenum Press, pp. 275-279
- Einhäupl K, Villringer A, Meister W, Mehrain S, Garner C, Pelkofer M, Haberl R, Pfister HW, Schmiedek P (1991) Heparin treatment in sinus venous thrombosis. *Lancet* 338:597-600
- Finger FW, Mook DG (1971) Basic drives. *Annu Rev Psychol* 22:1-38
- Fujita K, Kojima N, Tamaki N, Matsumoto S (1984) Brain edema in intracranial venous hypertension. In: *Brain Edema* (Inaba Y, Klatzo I, Spatz M, eds.), Berlin, Springer, pp. 228-234
- Gerhardt SC, Bernard PS, Pastor G, Boast CA (1986) Effects of systemic administration of the NMDA antagonist, CPP, on ischemic brain damage in gerbils. *Soc Neurosci Abstr* 12:59
- Gettelfinger DM, Kokmen E (1977) Superior sagittal sinus thrombosis. *Arch Neurol* 34:2-6
- Gloor P, Kalabay O, Giard N (1968) The electroencephalogram in diffuse encephalopathies: electroencephalographic correlates of grey and white matter lesions. *Brain* 91:779-802
- Gloor P, Ball G, Schaul N (1977) Brain lesions that produce delta waves in the EEG. *Neurology* 27:326-333
- Hanley DF, Feldman E, Borel CE, Rosenbaum AE, Goldberg AL (1988) Treatment of sagittal sinus thrombosis associated with cerebral hemorrhage and intracranial hypertension. *Stroke* 19:903-909
- Hassler O (1966) Deep cerebral venous system in man. A microangiographic study of its area of drainage and its anastomoses with superficial cerebral veins. *Neurology* 16:504-511
- Heinz ER, Geeter D, Gabrielsen TO (1972) Cortical vein thrombosis in the dog with a review of aseptic intracranial venous thrombosis in man. *Acta Rad Diag* 13:105-114
- Kingman TA, Mendelow AD, Graham DI, Teasdale GM (1988) Experimental intracerebral mass: description of model, intracranial pressure changes and neuropathology. *J Neuro-pathol Exp Neurol* 47:128-137
- Krayenbühl H (1966) Cerebral venous and sinus thrombosis. In: *Clinical Neurosurgery, Vol. 14* (Ojemann RG, Shillito J Jr, eds.), Baltimore, Williams and Wilkins, pp. 1-24
- Künkel H (1984) Pharmaco-electroencephalography—methods and problems. In: *Pain Measurements in Man. Neurophysiological Correlates of Pain* (Bromm B, ed.), Amsterdam, Elsevier, pp. 153-166
- Mattes W, Dörstelmann D (1981) Hirnvenen- und Sinusthrombose. Diagnose und Verlaufskontrolle der Antikoagulantientherapie durch Computertomographie. *Deutsche Med Wochenschr* 106:744-747
- Munderloh S, Schnapf D, Coker S, Citrin C (1981) Changing ventricular size in dural sinus thrombosis. *Comp Tomogr* 5:11-16
- Nag NK, Nadkarni ND (1971) Place of anticoagulant therapy in puerperal cerebral venous and venous sinus thrombosis. *J Ind. Med Assoc* 56:290-297
- Nagpal RD (1983) Dural sinus and cerebral venous thrombosis. *Neurosurg Rev* 6:155-160
- Owens G, Stahlman G, Capps J, Meirowsky AM (1957) Experimental occlusion of dural sinuses. *J Neurosurg* 14:640-647
- Paxinos G, Watson C (1986) *The Rat Brain Stereotaxic Coordinates*, Orlando, Florida, Academic Press
- Proctor RR, Papaport SI (1961) The partial thromboplastin time with kaolin: a simple screening test for first stage plasma clotting factor deficiencies. *Am J Clin Pathol* 36:212-219
- Pulsinelli WA, Brierley JB (1979) A new model of bilateral hemispheric ischemia in the unanesthetized rat. *Stroke* 10:267-272
- Putnam TJ (1935) "Encephalitis" and sclerotic plaques produced by venular obstruction. *Arch Neurol Psychiatr* 33:929-940
- Reddy CRRM, Rao MS (1968) Cerebral infarction due to intracranial venous sinus thrombosis. *J Ind Med Assoc* 50:98-102
- Sarwar M, Virapongse C, Carbo P (1984) Experimental production of superior sagittal sinus thrombosis in the dog. *Am J Neuroradiol* 6:19-22
- Sato S, Miyahara Y, Dohmoto Y, Kawase T, Toya S (1983) Cerebral microcirculation in experimental sagittal sinus occlusion in dogs. In: *The Cerebral Veins* (Auer LM, Loew F, eds.), New York, Springer, pp. 111-117
- Schumacher M (1984) Microangiographic study of the normal anatomy of the cerebral venous system in rats. *Neuroradiology* 26:137-140
- Sulg I (1984) Quantitative EEG as a measure of brain dysfunction. In: *Brain Ischemia: Quantitative EEG and Imaging Techniques, Progress in Brain Research, Vol. 62* (Pfurtscheller G, Jonkman EJ, Lopes da Silva FH, eds.), New York, Elsevier, pp. 65-84
- Ungersböck K, Heimann A, Kempfski O (1993) Cerebral blood flow alterations in a rat model of cerebral sinus thrombosis. *Stroke* 24:563-570
- Unterberg A, Wahl M, Baethmann A (1988) Effects of free radicals on permeability and vasomotor response of cerebral vessels. *Acta Neuropathol* 76:238-244
- Van Harreveld A (1972) The extracellular space in the vertebrate central nervous system. In: *The Structure and Function of Nervous Tissue, Vol. IV* (Bourne GA, ed.), New York, Academic Press, pp. 447-511
- Van Harreveld A, Ochs S (1956) Cerebral impedance changes after circulatory arrest. *Am J Physiol* 187:180-192
- Van Harreveld A, Murphy T, Nobel KW (1963) Specific impedance of rabbit's cortical tissue. *Am J Physiol* 205:203-207
- Wahl M, Young AR, Edvinsson L, Wagner F (1983) Effects of bradykinin on pial arteries and arterioles in vitro and in situ. *J Cereb Blood Flow Metab* 3:231-237
- Weber G (1966) Treatment of cerebral venous and sinus thrombosis. *Thromb Diath Haemorrh* 21:435-448
- West M, Parkinson D, Havlicek V (1982) Spectral analysis of the electroencephalographic response to experimental concussion in the rat. *EEG Clin Neurophysiol* 53:192-200
- Woolf AL (1954) Experimentally produced cerebral venous obstruction. *J Pathol Bact* 67:1-16
- Zeman W, Innes JRM (1963) *Craigie's Neuroanatomy of the Rat*, New York, Academic Press, pp. 30-41